

# Tunable comb filters and refractive index sensors based on fiber loop mirror with inline high birefringence microfiber

Wa Jin, Chao Wang, Haifeng Xuan, and Wei Jin\*

Department of Electrical Engineering, The Hong Kong Polytechnic University, Hong Kong, China

\*Corresponding author: eewjin@polyu.edu.hk

Received May 15, 2013; accepted September 15, 2013;  
posted September 19, 2013 (Doc. ID 190476); published October 17, 2013

Highly birefringent (Hi-Bi) microfiber-based fiber loop mirrors (FLMs) were studied for tunable comb filters and refractive index (RI) sensors. The use of two cascaded Hi-Bi microfibers instead of a single microfiber allows more flexibility in controlling the transmission/reflection characteristics of the FLM. The length of Hi-Bi microfibers is of the order of centimeters, one or even more than two orders of magnitude shorter than the conventional Hi-Bi fiber-based FLM devices. The transmission/reflection spectra are sensitive to the RI surrounding the microfibers, and RI sensitivity of 20,745 nm/RIU was experimentally demonstrated. © 2013 Optical Society of America

OCIS codes: (060.2420) Fibers, polarization-maintaining; (230.7408) Wavelength filtering devices; (060.2370) Fiber optics sensors.

<http://dx.doi.org/10.1364/OL.38.004277>

Microfiber/nanofiber photonic devices have attracted considerable interest recently. Optical fibers with diameters down to micrometer/nanometer scale have been made by tapering standard optical fibers or glass rods, and they have the potential of being used as low-loss air-clad microscale/nanoscale optical waveguides [1]. A number of microfiber/nanofiber devices have been reported, including coiled resonators [2], interferometers [3], filters [4], supercontinuum generation [5], and sensors [6].

Optical comb filters as multichannel filters have been studied intensively for application in wavelength division multiplexing (WDM) communication systems [7], and filters with flattop are particularly attractive for DWDM systems due to signal fidelity and tolerance of signal wavelength drift. Especially, all-fiber comb filters based on a Sagnac fiber loop mirror (FLM) are popularly used for all-optical signal processing and multiwavelength fiber lasers [8–10] due to lower insertion loss and better performance.

In this Letter, we investigate the use of highly birefringent (Hi-Bi) microfiber-based FLMs for tunable comb filters and high sensitivity refractive index (RI) sensors. Two different configurations are studied. One incorporates a single piece of twisted Hi-Bi microfiber in a Sagnac loop, while the other includes two pieces of Hi-Bi microfibers cascaded along a fiber with a rotation of their birefringence axes. This work on microfibers may result in novel applications, such as wavelength-scale light transmission and interconnection, which are useful for photonic integration, computing, and nanoscale sensing.

The Hi-Bi microfiber is made from a commercial SMF-28 (outer diameter  $D \sim 125 \mu\text{m}$ , core diameter  $d \sim 8.2 \mu\text{m}$ ,  $\Delta n \sim 0.36\%$ ) [11]. The SMF-28 fiber is first “processed” by use of a femtosecond IR laser system (Fig. 1) to cutting away parts of the silica cladding on opposite sides of the SMF, resulting in an approximately square-like cross section [inset (a) in Fig. 1]. Figure 2 shows photos of a “processed” SMF with a cutting

away depth of  $\sim 26 \mu\text{m}$ , and a length of  $\sim 3 \text{ mm}$ . The “processed” SMF is then taper-drawn to micrometer size by use of a flame-brushing technique. The cross-sectional shape of the “processed” region is well preserved during the initial taper-drawn process and eventually turns to an approximately elliptical shape when the fiber diameter is reduced down to wavelength scale, which generates a high birefringence of the order of  $10^{-2}$  [11], much bigger than conventional polarization maintaining fibers. The insertion loss of the tapered microfibers with diameter above  $2 \mu\text{m}$  is in general considerably smaller than 0.2 dB. The ellipticity depends on the depth of the cut and the parameters used in the tapering process.

To fabricate two cascaded Hi-Bi microfibers along the same SMF, the SMF is first cut at one location and the

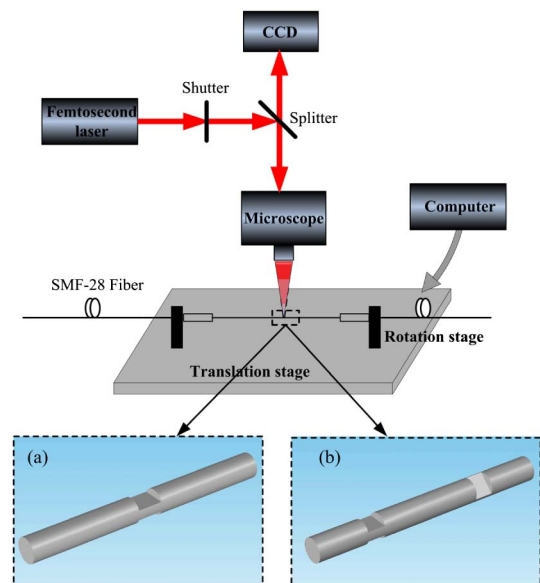


Fig. 1. Schematic of the femtosecond IR laser system. Insets: artistic view of the idealized “processed” SMF section to be tapered down to (a) a single Hi-Bi microfiber and (b) two cascaded Hi-Bi microfibers.

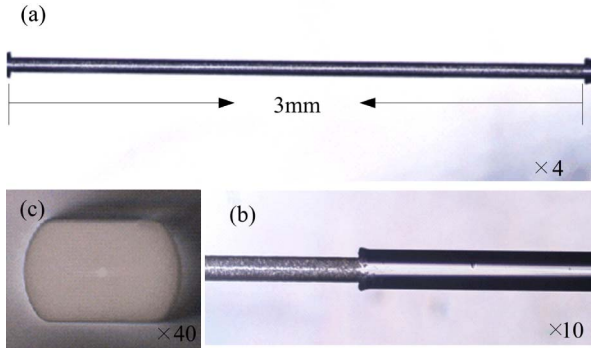


Fig. 2. Microscope images of (a) the entire “processed” SMF section, (b) side view, and (c) cross section of the “processed” section.

fiber is rotated by an angle  $\theta$  and moved longitudinally by 1 cm by use of a translation stage. The fiber is then cut at the second location, resulting in a “processed” fiber shown in the inset (b) of Fig. 1. The processed SMF is taper-drawn one section by one section, resulting in two Hi-Bi microfibers cascaded along the same SMF. A short section ( $\sim 3$  cm) of SMF is sandwiched between the two Hi-Bi microfiber sections and the angle between the birefringent axes of the two microfibers is  $\theta_2$ , which is equal to  $\theta$ .

By splicing the tapered microfiber into a Sagnac FLM, tunable comb filters and RI sensors may be made. The splice loss between the pigtails of the microfiber and the SMF forming the FLM is negligible because the microfiber is made on the same type of SMF. Figure 3 shows a FLM containing two cascaded sections of Hi-Bi microfibers (HB1 and HB2) with an angle  $\theta_2$  between their birefringent axes. The FLM also includes a polarization controller (PC) and a 50:50 SMF coupler. The incident light is split into clockwise and counterclockwise beams by the coupler, and the two beams pass through the PC and the Hi-Bi microfibers from opposite directions. The transmitted (T) and reflected (R) outputs may be expressed as [12]

$$T = \left[ \cos\left(\frac{\pi\Delta n_1 L_1 + \pi\Delta n_2 L_2}{\lambda}\right) \cos \theta_2 \sin(\theta_1 + \theta_3) + \cos\left(\frac{\pi\Delta n_1 L_1 - \pi\Delta n_2 L_2}{\lambda}\right) \sin \theta_2 \cos(\theta_1 + \theta_3) \right]^2, \quad (1)$$

$$R = 1 - T, \quad (2)$$

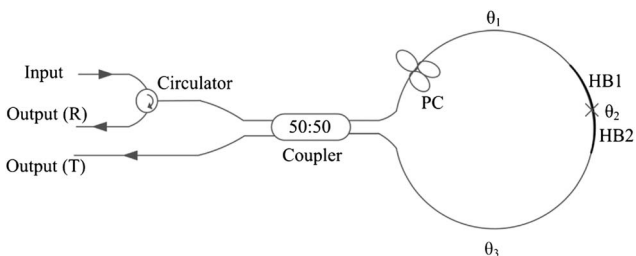


Fig. 3. Schematic diagram showing a FLM with two cascaded sections of Hi-Bi microfibers.

where  $\theta_1$  and  $\theta_3$  represent relative polarization angles and  $\Delta n_1$ ,  $\Delta n_2$  and  $L_1$ ,  $L_2$  are the birefringences and the lengths of the microfibers. For the case of a single microfiber,  $\theta_2$  and  $L_2$  become zero.

Figure 4(a) shows the measured transmission spectra of a FLM containing a 2 cm long Hi-Bi elliptical microfiber with a diameter of  $\sim 2.8$   $\mu\text{m}$  for its major axis, the insertion loss of this microfiber is less than 0.2 dB. The upper and lower curves are, respectively, for the microfiber placed in air and in water. From the upper curve birefringence of the microfiber is estimated to be about  $8.5 \times 10^{-3}$  [11] (at wavelength of 1550 nm). Because of the higher RI of water than air, the comb spacing is larger when the microfiber is immersed in water. During the experiments, the microfiber was kept straight by fiber holders and the transmission spectra were quite stable with no observable shift for a period of time at room temperature. By varying temperature, the RI of water can be changed. The temperature coefficient of water RI is of the order of  $\sim 1 \times 10^{-4}/^\circ\text{C}$ , and the value of the RI may be obtained from the lookup table in [13] once the temperature is known. Figure 4(b) shows the wavelength of a dip versus RI when the water temperature is varied from  $30^\circ\text{C}$  to  $80^\circ\text{C}$ , and the RI sensitivity obtained is  $\sim 20,788$  nm/RIU. The temperature sensitivity of the FLM with the microfiber placed in air is measured to be  $\sim 0.03$  nm/ $^\circ\text{C}$  at 1550 nm, indicating the wavelength shift is mainly due to the variation of water RI rather than the temperature.

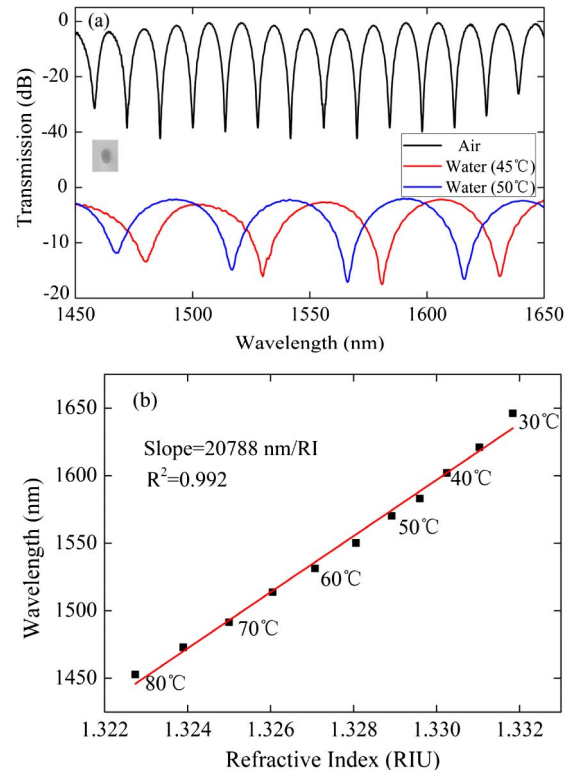


Fig. 4. (a) Transmission spectrum of a FLM containing one section of Hi-Bi microfiber. The inset shows the cross-sectional microscope image of the Hi-Bi microfiber. (b) Wavelength of a dip as a function of water RI when temperature is varied from  $30^\circ\text{C}$  to  $80^\circ\text{C}$ .

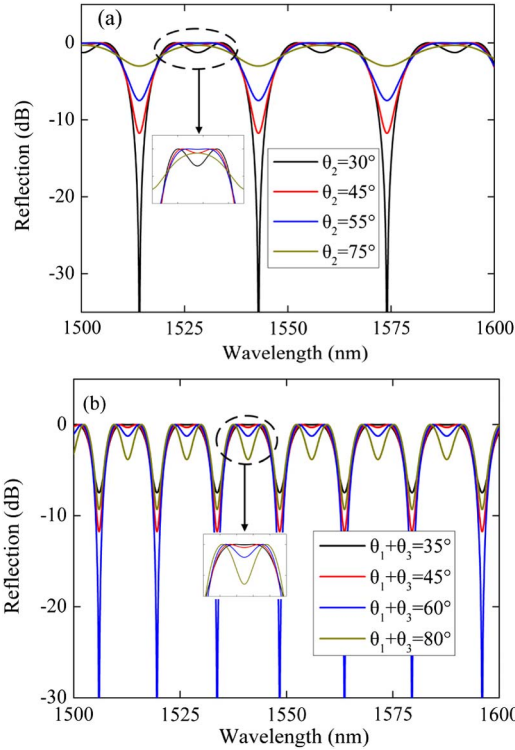


Fig. 5. Calculated reflection spectra for (a)  $L_1 = L_2 = 1$  cm,  $\theta_1 + \theta_3 = 60^\circ$  and (b)  $L_1 = L_2 = 2$  cm,  $\theta_2 = 30^\circ$ .

The use of two cascaded microfibers in a FLM would allow more flexibility in the design of comb filters. Figure 5 shows the calculated reflection spectra for two cascaded microfibers with different parameters. The calculation is based on Eqs. (1) and (2) with  $\Delta n_1 = \Delta n_2 = 8.5 \times 10^{-3}$  (at wavelength of 1550 nm). For Fig. 5(a), we used  $L_1 = L_2 = 1$  cm and  $\theta_1 + \theta_3 = 60^\circ$ , while the angle between the two Hi-Bi microfibers ( $\theta_2$ ) was varied from  $30^\circ$  to  $75^\circ$ . Figure 5(b),  $L_1 = L_2 = 2$  cm and  $\theta_2 = 30^\circ$  were used and  $\theta_1 + \theta_3$  was varied from  $35^\circ$  to  $80^\circ$ . From the calculated results, it can be seen that for the reflection spectra,  $\theta_2$  and  $\theta_1 + \theta_3$  affect the flatness of the wave top and the peak-to-notch contrast ratio while the birefringence and the length of Hi-Bi microfibers determines the channel spacing, indicating comb filters with desired properties may be designed by selecting the length and birefringence of the microfibers, as well as the angle of rotation of the birefringent axes.

Experiments were conducted with FLMs containing two cascaded Hi-Bi microfibers. The first FLM used one section 2 cm long tapered Hi-Bi microfiber with a  $55^\circ$  twist in the middle, equivalent to two cascaded 1 cm long microfibers with an angle between the birefringence axes of  $\theta_2 = 55^\circ$ . The cascaded microfiber sample was prepared by the following procedure. The 2 cm long Hi-Bi microfiber is fixed to the middle between two clamps with 12 cm separation between them, one of the clamps is fixed to a motor-driving rotation stage through which a 110 deg rotation is applied, as shown in Fig. 6(a). The CO<sub>2</sub> laser beam with a spot size of  $\sim 40$   $\mu\text{m}$  in diameter is scanned transversely across the fiber at the middle point between the clamps, resulting in local heating of the fiber and inducing a permanent twist of the fiber

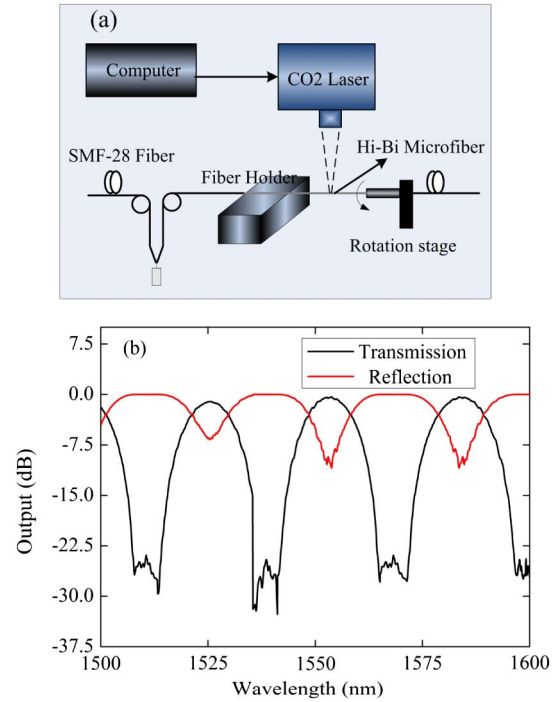


Fig. 6. (a) Experiment setup to twist one section of Hi-Bi microfibers and (b) transmission and reflection spectra.

at the midpoint with a twist angle  $\sim 55^\circ$ . The average power of the CO<sub>2</sub> laser was set to 0.015 W, which is sufficient to induce a permanent twist but with little

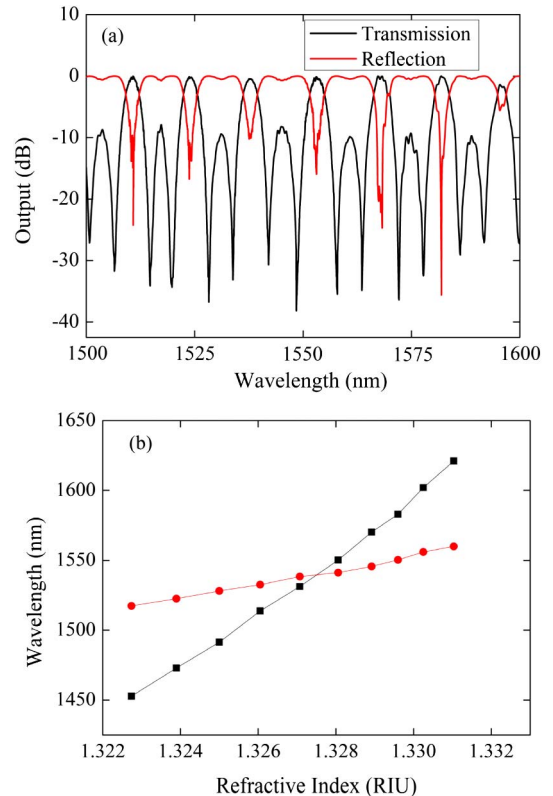


Fig. 7. (a) Measured transmission and reflection spectra for a FLM containing two cascaded Hi-Bi microfibers. (b) Wavelength of a dip as functions of RI. The RI variation is achieved by varying water temperature from  $30^\circ\text{C}$  to  $80^\circ\text{C}$ . One section (red circle) and both sections (black square) immersed in water.

deformation on the surface of the microfiber. The loss due to twist was found to be  $\sim 0.2$  dB.

The transmission and reflection spectra of this FLM are shown in Fig. 6(b), which agrees well with the calculated spectrum for  $\theta_1 + \theta_3 = 60^\circ$  and  $\theta_2 = 55^\circ$ . The comb filter has channel spacing of  $\sim 32$  nm and peak-to-notch contrast ratio of  $\sim 10$  dB. The response of this device to the RI was also measured and found to be 19,672 nm/RIU, which is similar to that of the single Hi-Bi microfiber without twist.

The second FLM contains two 2 cm long Hi-Bi microfibers made on the same SMF by the procedure described previously. The angle between the birefringent axes is  $30^\circ$ . Figure 7(a) shows measured transmission and reflection spectra of the second FLM, which is close to the calculated results for  $\theta_2 = 30^\circ$  and  $\theta_1 + \theta_3 = 60^\circ$ . The response of the FLM to external RI was also measured and the results are shown in Fig. 7(b). When both of the microfiber sections are immersed into water at the same time, the sensitivity of dip-wavelength to the RI was found to be  $\sim 20,075$  nm/RIU, similar to that of the FLM with a single microfiber. When only one of the microfiber sections is immersed into water, the sensitivity is 5036 nm/RIU, about 4 times lower.

In summary, FLMs containing a single Hi-Bi microfiber and two cascaded Hi-Bi microfibers are demonstrated for tunable comb filters and RI sensors. Compared with FLM comb filters made from conventional Hi-Bi fibers [12], the current devices need very short length of microfibers and the transmission/reflection spectra may be tuned by varying the RI surrounding the microfiber. The sensitivity of dip-wavelength to the RI was measured to be  $\sim 2 \times 10^4$  nm/RIU. The device could be useful for high sensitivity RI sensing, optical signal processing and

switching, power equalization, and management for WDM networks, especially for photonic integration, computing, and nanoscale sensing.

This work was supported by the Hong Kong SAR Government through a GRF grant PolyU5177/10E, and the Hong Kong Polytechnic University through grants G-YX5B and J-BB9K.

## References

1. L. M. Tong, R. R. Gattass, J. B. Ashcom, S. L. He, J. Y. Lou, M. Y. Shen, I. Maxwell, and E. Mazur, *Nature* **426**, 816 (2003).
2. X. S. Jiang, Y. Chen, G. Vienne, and L. M. Tong, *Opt. Lett.* **32**, 1710 (2007).
3. G. Salceda-Delgado, D. Monzon-Hernandez, A. Martinez-Rios, G. A. Cardenas-Sevilla, and J. Villatoro, *Opt. Lett.* **37**, 1974 (2012).
4. Y. Chen, Z. Ma, Q. Yang, and L. M. Tong, *Opt. Lett.* **33**, 2565 (2008).
5. S. Leon-Saval, T. Birks, W. Wadsworth, P. St. J. Russell, and M. Mason, *Opt. Express* **12**, 2864 (2004).
6. X. Fang, K. Demarest, H. Ji, C. T. Allen, and L. Pelz, *IEEE Photon. Technol. Lett.* **9**, 1490 (1997).
7. J. W. Wu, X. D. Tian, and H. B. Bao, *Prog. Electromagn. Res.* **76**, 127 (2007).
8. G. Y. Sun, D. S. Moon, A. X. Lin, W. T. Han, and Y. Chung, *Opt. Express* **16**, 3652 (2008).
9. S. Hu, L. Zhan, Y. J. Song, W. Li, S. Y. Luo, and Y. X. Xia, *IEEE Photon. Technol. Lett.* **17**, 1387 (2005).
10. G. Rossi, O. Jerphagnon, B. E. Olsson, and D. J. Blumenthal, *IEEE Photon. Technol. Lett.* **12**, 897 (2000).
11. H. Xuan, J. Ju, and W. Jin, *Opt. Express* **18**, 3828 (2010).
12. J. Wang, K. Zheng, J. Peng, L. Liu, J. Li, and S. Jian, *Opt. Express* **17**, 10573 (2009).
13. P. Schiebener, J. Straub, J. M. H. Levelt Sengers, and J. S. Gallagher, *J. Phys. Chem. Ref. Data* **19**, 677 (1990).